Separation of large scale water storage patterns over Iran using GRACE, altimetry and hydrological data

Remote Sensing of Environment

Volume 140, January 2014, Pages 580–595

Separation of large scale water storage patterns over Iran using GRACE, altimetry and hydrological data, Journal of Remote Sensing of Environment, 140, Pages 580-595, dx.doi.org/10.1016/j.rse.2013.09.025.

E. Forootan[a], R. Rietbroek[a], J. Kusche[a], M. A. Sharifi[b], J. L. Awange[c], M. Schmidt[d], P. Omondi[e], J. Famiglietti[f]

[a] *Institute of Geodesy and Geoinformation (IGG), Bonn University, Bonn, Germany*
[b] *Surveying and Geomatics Engineering Department, University of Tehran, Iran*
[c] *Western Australian Centre for Geodesy and The Institute for Geoscience Research, Curtin University, Perth, Australia*
[d] *German Geodetic Research Institute (DGFI), Munich, Germany*
[e] *IGAD Climate Prediction and Applications Centre (ICPAC), Nairobi, Kenya*
[f] *UC Center for Hydrologic Modeling, University of California, Irvine, CA, USA*

Abstract

Extracting large scale water storage (WS) patterns is essential for understanding the hydrological cycle and improving the water resource management of Iran, a country that is facing challenges of limited water resources. The Gravity Recovery and Climate Experiment (GRACE) mission offers a unique possibility of monitoring total water storage (TWS) changes. An accurate estimation of terrestrial and surface WS changes from GRACE-TWS products, however, requires a proper signal separation procedure. To perform this separation, this study proposes a statistical approach that uses a priori spatial patterns of terrestrial and surface WS changes from a hydrological model and altimetry data. The patterns are then adjusted to GRACE-TWS products using a least squares adjustment (LSA) procedure, thereby making the best use of the available data. For the period of October 2002 to March 2011, monthly GRACE-TWS changes were derived over a broad region encompassing Iran. A priori patterns were derived by decomposing the following auxiliary data into statistically independent components: (i) terrestrial WS change outputs of the Global Land Data Assimilation System (GLDAS); (ii) steric-corrected surface WS changes of the Caspian Sea; (iii) that of the Persian and Oman Gulfs; (iv) WS changes of the Aral Sea; and (v) that of small lakes of the selected region. Finally, the patterns of (i) to (v) were adjusted to GRACE-TWS maps so that their contributions were estimated and GRACE-TWS signals separated. After separation, our re-

Email addresses: forootan@geod.uni-bonn.de (E. Forootan), roelof@geod.uni-bonn.de (R. Rietbroek), kusche@geod.uni-bonn.de (J. Kusche), sharifi@ut.ac.ir (M. A. Sharifi), J.Awange@curtin.edu.au (J. L. Awange), M. Schmidt: schmidt@dgfi.badw.de (M. Schmidt), philip.omondi@gmail.com (P. Omondi), jfamigli@uci.edu (J. Famiglietti)

sults indicated that the annual amplitude of WS changes over the Caspian Sea was 152 mm, 101 mm over both the Persian and Oman Gulfs, and 71 mm for the Aral Sea. Since January 2005, terrestrial WS in most parts of Iran, specifically over the center and northwestern parts, exhibited a mass decrease with an average linear rate of $\sim$ 15 mm/yr. The estimated linear trends of groundwater storage for the drought period of 2005 to March 2011, corresponding to the six main basins of Iran: Khazar, Persian and Oman Gulfs, Urmia, Markazi, Hamoon, and Srakhs were -6.7, -6.1, -11.2, -9.1, -3.1, and -4.2 mm/yr, respectively. The estimated results after separation agree fairly well with 256 in-situ piezometric observations.

Keywords: GRACE-TWS, Signal separation, Independent components, Terrestrial and surface water storage, Groundwater, Iran

1. Introduction

Water resource of the Islamic Republic of Iran (Iran) is under pressure due to population growth, urbanization and its related consequences (FAO, 2009). The direct impact of the increasing population ($\sim$ 75 million in 2010) on water resources resulted in increased need for fresh water in populated centers, while its indirect impact was an increase in demand of agricultural land and development of irrigation lands (e.g., Ardakani, 2009). Sarraf et al. (2005) state that the total water resources per capita in Iran plunged by more than 65% since 1960, and a decrease of 16% is expected by 2025. The increased demand for groundwater, on one hand, and the high rate of irrigation and over-exploitation of water resources in some areas on the other hand are also likely to become a serious challenge for future protection of groundwater basins of central and northern Iran (Motagh et al., 2008; Mohammadi-Ghaleni and Ebrahimi, 2011).

Since 90% of Iran is located in arid or semi-arid areas, the direct rainfall is its only water recharge. This means that only 10% of the country receives enough rainfall to meet its need while the other much drier parts are heavily dependent on groundwater. Using Synthetic-Aperture Radar (SAR) data, Motagh et al. (2008) showed a land subsidence related to groundwater storage extractions in the central part of Iran between 1971 and 2001. Combining precipitation data with measured piezometric groundwater levels, Van Camp et al. (2012) pointed out that there is an imbalance between exploitation and precipitation recharge in central Iran, which has resulted in the decline of water storage (WS). Their study, however, was restricted to the Shahrekord aquifer (located at $\sim$ [32.3°N] and [50.9°E]).

Such conditions, therefore, justify the exploration of alternative monitoring tools that can provide reliable information to improve water policies. These are needed in the management of drought and flood related impacts, as well as improving the overall water situation in the region. Among different hydrological parameters, total water storage (TWS), defined as the summation of all water masses in the Earth's storage compartments (atmosphere, surface waters, ground water, etc.), is an important indicator of the water cycle (Güntner,

2008). TWS changes can also be used for evaluating the past and present state of natural resources such as water and fodder, as well as for modeling their future development within the context of human usage and climate change (see e.g., Becker et al., 2010; Grippa et al., 2011; Forootan et al., 2012).

For a long time, mapping of terrestrial WS changes mainly relied on piezometric observations, in-situ meteorological measurements, as well as hydrological modeling approaches. Although such approaches are very important for understanding the mechanism of water cycle, they are limited e.g., by data inconsistencies, spatial and temporal data gaps or instrumental and human errors and oversights (Rodell et al., 2007). For Iran, specifically, most of the previous studies focused only on regional water variations, see e.g., Ghandhari and Alavi-Moghaddam (2011). Using such local studies, it is difficult to assess the large scale heterogeneity of the terrestrial water cycle, due to the vast climate and topographic condition of the country (see, e.g., Section 2 and Modarres, 2006). Other studies that looked at the large-scale water variations of Iran were restricted to the use of hydrological models (e.g., Abbaspour et al., 2009; Noory et al., 2011).

Since March 2002, however, the Gravity Recovery and Climate Experiment (GRACE) is routinely providing satellite-based estimates of changes in TWS within the Earth's system (see e.g., Tapley et al., 2004a,b; Wahr et al., 2004; Kusche et al., 2012; Famiglietti and Rodell, 2013). GRACE-TWS have been used to study regional patterns of TWS changes, e.g., over Asia (e.g., Rodell et al., 2009; Shum et al., 2011; Schnitzer et al., 2013), Africa (e.g., Awange et al., 2013; Becker et al. 2010; Grippa et al., 2011), Australia (e.g., Awange et al., 2011; Van Dijk et al., 2011; Forootan et al., 2012). On a global scale, TWS changes are discussed e.g., in Syed et al. (2008), and Forootan and Kusche (2012). All these studies came to the same conclusion that GRACE-TWS products are suitable for studying large scale WS changes on annual and inter-annual time scales.

Studies which address TWS changes of the regions around Iran include, for example, the works of Swenson and Wahr (2007) who used satellite altimetry (Jason1) together with GRACE monthly gravity solutions to analyze the WS changes of the Caspian Sea from mid 2002 to 2006, and provided a multi-sensor monitoring of the sea. Avsar and Ustun (2012) showed a downward linear trend of GRACE derived gravity changes over a region including Turkey and west of Iran from 2003 to 2010. Studies of Llovel et al. (2010) and Baur et al. (2013) addressed the basin averaged TWS changes of the Volga River Basin (located in Russia), as well as Tigris-Euphrates region in Iraq. In the same region, Longuevergne et al. (2012) evaluated water variations within the Tigris-Euphrates reservoirs and found a decrease of $\sim$ 17 km^3 during the drought period between 2007 and 2010. In a recent study, Voss et al. (2013) showed that the pattern of the water loss is extending into the northwestern Iran including the Urmia Basin (see basin 3 in Fig. 1). They also reported that the strong decline of water storage was most likely caused by groundwater depletion in this region between 2003-2009. Our contribution extends these previous studies by looking at the recent patterns of WS changes (from October 2002 to March

2011) over the main basins of Iran.

Estimating accurate terrestrial or surface WS changes from GRACE-TWS products, however, requires a signal separation approach (e.g., Schmidt et al., 2008; Forootan and Kusche, 2012; Schmeer et al., 2012). This is due to the fact that: (a) GRACE time-variable gravity field products exhibit correlated errors at high degrees (e.g., Swenson and Wahr, 2006; Kusche, 2007; Klees, 2008) that need to be reduced; and (b) GRACE-TWS products represent a mass integral which needs to be separated into their compartments. i.e. the mass variations within Earth's interior or on its surface or atmosphere. Regarding (a), it is common to apply a filter before computing TWS changes from GRACE time-variable gravity products (e.g., Kusche, 2007). Nevertheless, this filtering introduces biases in the mass change estimations since the mass anomalies are smeared out and moved due to the spatial filtering, known as the 'leakage' problem (Swenson and Wahr 2002; Klees, 2007). Fenoglio-Marc et al. (2006; 2012) and Longuevergne et al. (2010) show that the leakage is larger for regions where land meets water reservoirs such as lakes, seas and oceans and also for small basins. To account for these leakages, most of the previous studies focused on basin-wide approaches (e.g., Fenoglio-Marc et al., 2006; 2012; Llovel at al., 2010; Longuevergne et al., 2010; Baur et al., 2013; and Jensen et al., 2013). However, due to the vast size of our region of study, and its varying climatic conditions (see Section 2), it is desirable to implement information extraction methods that allow the retrieval of spatially varying WS changes. This capability is a feature that is usually lost when one applies basin-wide averaging methods.

Regarding (b), one may assume that the main source of GRACE-TWS variability consists of the contribution of the terrestrial and surface WS changes (Güntner et al., 2007). We assume that the ocean and atmospheric mass variations have already been removed from GRACE time-variable solutions using de-aliasing products (Flechtner, 2007a,b). Although, this procedure in itself might introduce some errors in TWS estimations (see, e.g., Duan et al., 2012; Forootan et al., 2013), that is not considered in this paper. For partitioning GRACE-TWS, most of the previous studies use altimetry observations to account for the surface WS changes (e.g., Swenson and Wahr, 2007; Becker et al., 2010) and hydrological models for terrestrial water changes (e.g., Syed et al., 2005; Rodell et al., 2007; Van Dijk, 2011; Van Dijk et al., 2011). Subsequently, GRACE-TWS signals are compared or reduced with altimetry and/or model derived WS values. The accuracy of the estimation in such approaches might be limited since, for instance, altimetry observations contain relatively large errors over inland waters (e.g. Birkett, 1995; Kouraev et al., 2011) and hydrological models show limited skill (e.g., Grippa et al., 2011; Van Dijk, 2011).

In this study, however, instead of removing those surface and terrestrial WS (respectively derived from altimetry and hydrological models) from GRACE-TWS maps, we use them as a priori information, to introduce the spatial patterns of surface and terrestrial WS changes. Then GRACE-TWS signals are separated by adjusting the derived spatial patterns to GRACE-TWS maps. For this means, TWS data within a rectangular box (between [23° to 48°N] and [42° to 63°E]) that includes Iran, is extracted from each monthly GRACE-TWS

map. As mentioned before, the main source of TWS variability, within each map, consists of the contribution of the terrestrial and surface WS changes (Güntner et al., 2007). In our case, the surface water variations are mainly caused by water reservoirs within the selected box e.g., the Caspian Sea, Persian and Oman Gulfs, Aral Sea as well as other small lakes. Note that the effect of self-gravitational forces, other than those of surface and terrestrial WS changes, might be considerable over the region. A discussion can be found in Appendix B.

The higher-order statistical method of independent component analysis (ICA) (Forootan and Kusche, 2012; 2013) is used to identify statistically independent patterns from (i) monthly WS outputs of the Global Land Data Assimilation System (GLDAS) model (Rodell et al., 2004) over the selected rectangular box; (ii) Surface WS changes derived from altimetry observations of Jason1&2 missions over the Caspian Sea; (iii) sea surface heights (SSH)s in the Persian and Oman Gulfs after removing steric sea level changes; (iv) surface WS changes in the Aral Sea; as well as (v) the other main lakes of the selected box. The derived independent patterns of (i) to (v) were used as known spatial patterns (base-functions) in a least squares adjustment (LSA) procedure, to separate GRACE-TWS maps. This procedure gives the opportunity to make the best use of all available data sets in a LSA framework. A similar argument has been pointed out e.g., in Schmeer et al. (2012), who used experimental orthogonal functions of geophysical models in a LSA model for separating global GRACE integral signals. After separation, besides adjusting the terrestrial WS of (i) to GRACE-TWS, and the estimation of surface WS changes of the region (ii to v), for the first time, our study offers changes of the groundwater within the six main basins of Iran (basins are shown in Fig. 1). Our results are also compared with in-situ piezometric measurements.

The remaining part of the paper is organized as follows: in Section 2, we briefly describe the study region. The data used in the study is presented in Section 3. Section 4 outlines the analysis methods, and the results of separation are presented and discussed in Section 5. Finally, Section 6 concludes the paper and provides an outlook. The paper also includes two appendices that provide the results of ICA applied on GLDAS and altimetry derived WS changes (Appendix A), and the effect of self-gravitation on the results (Appendix B).

2. The Study Region

2.1. Geography

Iran with an area of about 1.7 million km^2 lies between latitudes [24° to 40°N] and longitudes [44° to 64°E] (Fig. 1). The landscape of Iran is dominated by rugged mountain ranges that separate various basins from each other. The largest mountain chain is that of the Zagros, which runs from the northwest of the country southwards to the shores of the Persian Gulf and then continues eastwards along most of the southeastern province. Alborz is the other main

mountain chain range that runs from the northwest to the east along the southern edge of the Caspian Sea. Over 50% of the area between the two main chains are covered by salty swamps of Dasht-e-Kavir and Dasht-e-Lut.

2.2. Basins and Climate

According to FAO (2009), there are 6 main catchments in Iran (i.e. Fig. 1) that include, the Central Plateau in the centre (basin 4; Markazi), the Lake Urmia Basin in the northwest (basin 3), the Persian and Oman Gulf basins in the west and south (basin 2), the Lake Hamoon Basin in the east (basin 5), the Kara-Kum Basin in the northeast (basin 6; Sarakhs) and the Caspian Sea Basin in the north (basin 1; Khazar). All these basins, except the Persian and Oman Gulf Basin, are interior. The Markazi basin, covering over half of the area of the country, has less than one third of the total renewable water resources (FAO, 2009). Shapes of the basins, their areas, and the percentage of their renewable water resources are summarized in Fig. 1.

The climate of Iran is quite extreme. Its northern edge is categorized as subtropical region (Khazar basin in Fig. 1). Whereas the climate of the other parts, i.e. 90% of the country, ranges from arid to semiarid, with extremely hot summers in central and the southern coastal regions. The main source of the input water in Iran is annual precipitation. The highest annual rainfall of 2275 mm has been recorded in Rasht, located near the Caspian Sea. Annual rainfall is less than 50 mm in the deserts (FAO, 2009).

2.3. Main Surface Waters of the Region

The Caspian Sea

The Caspian Sea, with an area of $\sim 371{,}000\ km^2$ is the world's largest inland water body (Kosarev and Yablonskaya, 1994). Kouraev et al. (2011) provide a detailed description on the geographical and physical aspects of the Caspian Sea. The Caspian Sea exhibits considerable fluctuations in its water levels, which have been the subject of several studies (e.g., Kouraev et al., 2011; Sharifi et al., 2013). Using a point-wise technique, Sharifi et al. (2013) illustrated that due to the vast size of Caspian, the varying climatic patterns within the whole sea, and the large impact of the Volga River, each region of the sea is expected to have a water level pattern different from the other regions. Their results indicate that during June 2001 to December 2005 and January 2006 to October 2008, linear rates of level variations are respectively 106 and -161 mm/yr. The extreme temperature conditions of the sea also contribute to the changing of the sea level, which exhibits an annual amplitude of $\sim$ 20 mm (e.g., Swenson and Wahr, 2007).

Urmia Lake

Lake Urmia (located in the Urmia Basin of Fig. 1, $\sim$ [37.7°N and 45.31°E]) is a salty lake with a surface area of $\sim 5000\ km^2$ (year 2000). The area of the lake is shrinking, which is partly due to the decade-long drought of its watershed and also due to the construction of 35 dams (since the 1990's) on the rivers

208 which feed the lake. Crétaux et al. (2011) provided altimetry and imagery
209 results for Lake Urmia (e.g., http://www.legos.obs-mip.fr/en/soa/hydrologie/
210 hydroweb/Page_ 2.html).

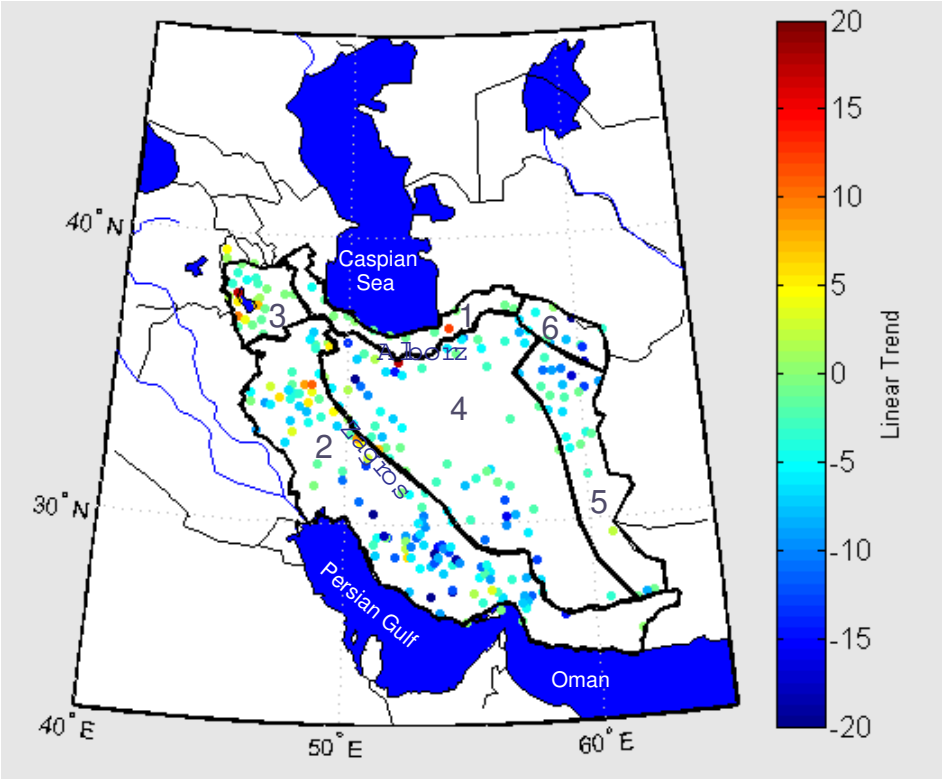

Major Basins of Iran	Percentage of total area of the country	Percentage of total renewable water resources	Number of Stations	Mean of Linear Trend of 2003-2010
1) Khazar	10	15	24	-6 mm/yr
2)Persian and Oman Gulfs	25	46	91	-5 mm/yr
3)Urmia	3	5	19	-13 mm/yr
4)Markazi	52	29	103	-2.5 mm/yr
5)Hamoon	7	2	12	-1.1 mm/yr
6)Sarakhs	3	3	7	-2.3 mm/yr

Figure 1: An overview of in-situ groundwater stations within the six major basins of Iran. The definition of the basins, their areas and renewable water resource percentages are according to FAO (2009). In-situ observations are provided by the Iranian Water-Resource Research Center. The linear rate of water storage change are computed using a least squares approach, while considering the annual and semi-annual frequencies. The Caspian and Aral Sea as well as the Persian and Oman Gulfs are masked out in blue.

The Persian Gulf and the Gulf of Oman

The Persian Gulf, with a surface area of $\sim$ 251,000 km^2, is a shallow water body in the south (see Fig. 1). Since the Gulf region is surrounded by arid land masses, it has strong seasonal and even daily air temperature fluctuations. Air temperature can drop to $0°C$ in winter and reach up to $50°C$ in summer (Kampf and Sadrinasab, 2006), which can contribute to the level fluctuations. Long-term observations of sea level also shows a rise at the head of the Persian Gulf, located in the Tigris-Euphrates delta of southern Iraq and the adjacent regions of southwestern Iran. Lambeck et al. (2002) linked this rise to post glacial rebound.

The Gulf of Oman connects the Arabian Sea to the Persian Gulf via the strait of Hormuz. The waters of the Gulf of Oman have more oceanic characteristics than those of the Persian Gulf. However, this does not make the fluctuation of the Gulf greater than the Persian Gulf. Hydrology and circulation aspects of the Oman Gulf are discussed e.g., in Pous et al. (2004).

3. Data

Four main datasets for the period of 2002 to 2011 were used in this study. These are (a) monthly TWS variations derived from GRACE, (b) surface WS changes derived from satellite altimetry observations, (c) terrestrial WS changes from GLDAS, and (d) 256 in-situ piezometric observations covering the six main basins of Iran. In addition, maps of sea surface temperature (Reynolds et al., 2002) and steric sea level (Ishii and Kimoto, 2009) variations are also used to reduce the contribution of temperature and salinity changes from altimetric SSHs, while converting them to surface WS changes. Note that surface WS is commonly called equivalent water height (EWH) in other studies.

3.1. GRACE

GRACE, a joint German/USA satellite project, was launched in March 2002 to detect mass variations within the Earth's system. In this work, we examined monthly GFZ release 04 gravity field solutions provided by the German Research Centre for Geosciences (GFZ) (Flechtner, 2007b). The data was computed up to degree and order 120 and cover the period from October 2002 to March 2011. GRACE degree 1 coefficients have been augmented by the results of Rietbroek et al. (2009) in order to include the variation of the Earth's center of surface figure with respect to the Earth's centre of mass, in which GRACE products have been computed. We also replaced the zonal degree 2 spherical harmonic coefficients (C_{20}) by values obtained from satellite laser ranging (SLR) (Cheng and Tapley, 2004), which were obtained from the GRACE Tellus Team website (grace.jpl.nasa.gov).

GRACE time-variable products contain correlated errors, manifesting itself as a striping pattern (Kusche, 2007). In order to remove the stripes, we applied the de-correlation filter of DDK2 (Kusche et al., 2009) to the GFZ solutions. The choice of the DDK2 filter, which is an anisotropic filter, arises from the

consistent results with respect to the outputs of hydrological models (Werth et al., 2009). Before computing monthly TWS fields, residual gravity field solutions with respect to the temporal average over the study period were computed. The residual coefficients were then transformed into $0.5^\circ \times 0.5^\circ$ TWS maps using the approach in Wahr et al. (1998). A rectangular box between ([23° to 48°N] and [42° to 63°E]) was then extracted from the monthly TWS grids. For the region of interest, the gridded Root-Mean-Square (RMS) of the GRACE-TWS signals is shown in Fig. 2,A. Strong anomalies are visible over the Caspian Sea, Lake Urmia, as well as over parts of the Zagros and Alborz mountains. The large RMS of the signal over the Caspian Sea and the mountains are due to the strong seasonality of TWS changes. Over Urmia, the strength of the GRACE-derived storage signal is mainly due to the water loss of the lake (see e.g., Voss et al., 2013).

3.2. Altimetry Data

We used monthly gridded altimetry data over the rectangular region mentioned above (including the Caspian Sea, the Aral Sea, the Persian and Oman Gulfs, and Urmia Lake as well as other small lakes and reservoirs), covering 2002 to 2011.3. Sea surface heights (SSH)s were originally produced by AVISO and provided through NOAA ERDDAP (the Environmental Research Division's Data Access Program program, see http://coastwatch.pfeg.noaa.gov/erddap/griddap/noaa_pifsc_9c36_df47_3dd4.html). The RMS of the altimetry signals is shown in Fig. 2,B. For the Caspian Sea, which has the dominant impact on the GRACE-TWS signals over the region, we compared NOAA's SSH with the gridded results of Sharifi et al. (2013), and obtained a correlation of 0.91 for the period of 2002 to 2010.

Water level fluctuations derived from altimetry can be compared to GRACE results, when they are corrected for the so called steric or volumetric height variations caused by temperature and salinity changes (Chambers, 2006). From the areas that contain surface water in this study, the levels of the Caspian Sea and the Persian and Oman Gulfs exhibit a considerable steric component. We used monthly steric sea level changes of Ishii and Kimoto (2009) to convert SSH of the Persian and Oman Gulfs to surface WS changes. Since Ishii and Kimoto (2009)'s study does not cover the Caspian Sea, we followed the approach of Swenson and Wahr (2007) by using SST (sea surface temperature) data and taking a conversion factor of 8.43 mm/yr to convert them to steric sea level changes over the Caspian Sea. The SST data, used here, were reconstructed Reynolds et al. (2002) SST maps obtained from the United States (US) National Oceanic and Atmospheric Administration (NOAA) official website (http://www.esrl.noaa.gov/psd/data/gridded/ data.ncep.oisst.v2.html). Each map of SSH (after reducing the steric part) was filtered using the same DDK2 filter as applied to the GRACE-TWS maps. After applying the DDK2 filter on surface WS data, the mean damping ratio of the filtered data to the original values was ~ 0.71.

3.3. GLDAS Model

The GLDAS hydrological model integrates a large quantity of observed data and modeling concepts (Rodell et al., 2004) to produce a global hydrological model. GLDAS terrestrial WS data for the period of study were obtained from the Goddard Earth Sciences Data and Information Services Center (http://grace.jpl.nasa.gov/data/gldas/). Consequently, terrestrial WS considered here constitutes of total column soil moisture (TSM), Snow Water Equivalent (SWE) and Canopy Water Storage (CWS). Groundwater storage changes are not represented in the GLDAS model simulations. As a result, our a priori pattern of the terrestrial storage partitioning is limited, and might not include a complete description of the lateral and vertical distribution of water storage up to the surface (see e.g., Rodell and Famiglietti, 2001; Syed et al., 2008). The GLDAS-WS data were filtered by the same DDK2 filter in order to match the signal content of the GRACE-TWS fields. The RMS of GLDAS data for the mentioned rectangular box is shown in Fig. 2,C. The results show strong signals over the northwest of the country and over the Zagros and Alborz mountains. The strength of the signal is due to the strong annual variability of TWS over these regions. We compared the mean magnitude of the DDK2-filtered GLDAS data with its original values over the region and found a damping ratio of ~ 0.83 due to the filter.

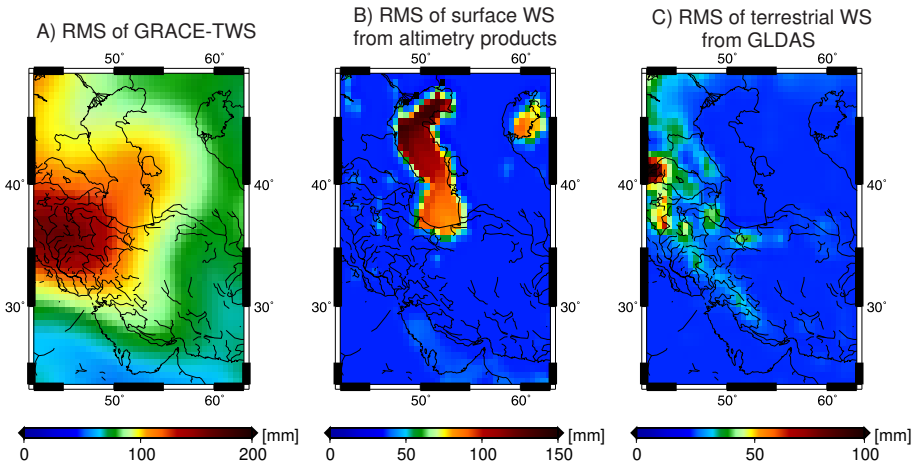

Figure 2: The signal strength (RMS) of the three main data sets used in this study after smoothing using Kusche et al. (2009)'s DDK2 filter; (A) GRACE-TWS data, (B) surface WS from altimetry data and (C) terrestrial WS output of the GLDAS model.

3.4. In-situ Piezometric Measurements

This study used in-situ groundwater observations of 256 selected piezometric stations of the Iranian Water-resource Research Center, of which 24, 91, 19, 103, 12 and 7 stations are located in the basins one to six of Fig. 1, respectively. The observations cover the period 2003 to 2010 and have been tested for their quality

in terms of outliers and possible biases. The location of the stations and their computed linear trends for 2003 to 2010 are shown in Fig. 1. In agreement with the other data, most parts of Iran exhibited a WS decline during the mentioned period. Note that, there jumps exist in the in-situ time series as a result of water network changes. Their impact on the computed trends will be addressed in Section 5.2.

4. Methodology

Monthly GRACE-TWS maps, used in this study (ocean and atmospheric mass variations are already removed), reflect an integral measure of the combined effect of terrestrial WS changes of land hydrology (H), and surface WS changes of seas, lakes and reservoirs (R). Assuming that GRACE-TWS fields are stored in a matrix $\mathbf{T} = \mathbf{T}(s,t)$, where t is the time, and s stands for spatial coordinate (grid points). $\mathbf{T}$ can be factorized into spatial and temporal components (Schmeer et al., 2012) as

$$\mathbf{T} = \mathbf{C}_H \mathbf{A}_H^T + \mathbf{C}_R \mathbf{A}_R^T, \tag{1}$$

where $\mathbf{C}_{H/R} = \mathbf{C}_{H/R}(t)$ and $\mathbf{A}_{H/R} = \mathbf{A}_{H/R}(s)$ are respectively the temporal and spatial patterns (base-functions). We used H and R as subindices to show the base-functions that are computed from terrestrial WS (H) and surface WS (R). In Eq. 1, $\mathbf{C}_H$ contains zero over the gridpoints of surface water and $\mathbf{C}_R$ contains zeros over the land.

In Eq. 1, once either of $\mathbf{C}_{H/R}(t)$ or $\mathbf{A}_{H/R}(s)$ is determined, the other component can be computed by solving a LSA. Schmeer et al. (2012) used a similar approach for separating global GRACE-TWS integral into its atmospheric, hydrologic and oceanic contributors. Their study suggests the application of a statistical decomposition method on the data/model of each compartment to compute the required base-functions of Eq. 1. Accordingly, we follow their approach and use steric corrected SSHs and the WS output from the GLDAS model as described in Section 3 to compute the required $\mathbf{C}_{H/R}$ and $\mathbf{A}_{H/R}$.

ICA, an extension of the second-order statistical method of principal component analysis (PCA) (Preisendorfer, 1988), allows the extraction of statistically independent patterns from spatio-temporal data sets (Cardoso and Souloumiac, 1993). Applications of ICA for filtering (Frappart et al., 2010) and decomposition of GRACE-TWS are discussed e.g., in Forootan and Kusche (2012; 2013) and Forootan et al. (2012). Of the two alternative ways of applying ICA, in which either temporally independent components or spatially independent components are constructed (Forootan and Kusche, 2012), we used temporal ICA. The motivation of this selection was based on the intentions of the study, which focuses on signals which have distinct temporal behaviour (e.g., seasonal and trend of water changes). The temporal ICA method is simply called ICA in this paper, and the decomposition of the centered (temporal mean removed) time series of $\mathbf{H}$ and $\mathbf{R}$ is written as

$$\mathbf{H}= \bar{\mathbf{P}}_H \hat{\mathbf{R}}_H \hat{\mathbf{R}}_H^T \mathbf{E}_H^T = \mathbf{C}_H {\mathbf{A}_H}^T, \tag{2}$$

and

$$\mathbf{R}= \bar{\mathbf{P}}_R \hat{\mathbf{R}}_R \hat{\mathbf{R}}_R^T \mathbf{E}_R^T = \mathbf{C}_R {\mathbf{A}_R}^T. \tag{3}$$

As stated in Forootan and Kusche (2012), $\bar{\mathbf{P}}_{H/R}$ and $\mathbf{E}_{H/R}$ contain orthogonal components in their columns that are derived by applying PCA on the centered data sets of $\mathbf{H}$ and $\mathbf{R}$ (Preisendorfer, 1988). In Eqs. 2 and 3, T is a transpose operator, $\bar{\mathbf{P}}_{H/R}$ is normalized (i.e. $\bar{\mathbf{P}}_{H/R}\bar{\mathbf{P}}_{H/R}^T = \mathbf{I}$), $\hat{\mathbf{R}}_{H/R}$ is an optimum rotation matrix that rotates the temporal components of $\bar{\mathbf{P}}_{H/R}$ to make them temporally as mutually independent as possible (Forootan and Kusche, 2012).

As a result of the temporal ICA decomposition, $\mathbf{C}_{H/R} = \bar{\mathbf{P}}_{H/R}\hat{\mathbf{R}}_{H/R}$ contains statistically mutually independent temporal components. $\mathbf{A}_{H/R} = \bar{\mathbf{E}}_{H/R}\hat{\mathbf{R}}_{H/R}$ stores their corresponding spatial maps, that are still orthogonal. $\mathbf{A}_{H/R}$, therefore, will be used in Eq. 1 as known spatial patterns and a new temporal expansions of $\hat{\mathbf{C}}_{H/R}$ will be computed using the LSA approach (e.g., Koch, 1988),

$$[\hat{\mathbf{C}}_H\ \hat{\mathbf{C}}_R]^T = \Big[[\mathbf{A}_H\ \mathbf{A}_R]^T[\mathbf{A}_H\ \mathbf{A}_R]\Big]^{-1}\ [\mathbf{A}_H\ \mathbf{A}_R]^T\ \mathbf{T}^T. \tag{4}$$

In Eq. 4, $\hat{\mathbf{C}}_{H/R}$ contains adjusted temporal components over the land and surface waters and $\mathbf{T}$ contains GRACE-TWS observations. Then, $\hat{\mathbf{C}}_H$ and $\hat{\mathbf{C}}_R$ can be respectively replaced in Eqs. 2 and 3 to reconstruct terrestrial WS changes over the land and surface WS changes.

5. Numerical Results

5.1. Comparison of GRACE and altimetry

From Fig. 2,A, the strongest variability during 2002-2011 detected by GRACE is concentrated over Urmia Lake and the Caspian Sea. Before implementing the separation approach described in Section 4, we first compared the averaged volume variations of Urmia and the Caspian Sea derived from GRACE with those of satellite altimetry. For deriving the time series of the Urmia Basin, we took the boundary of basin (3) in Fig. 1 as our reference. A basin-averaged TWS was computed for Urmia Lake using a similar approach to that of Swenson and Wahr (2007), which is the dash-black line in Fig. 3,A. Then, the contribution of terrestrial WS surrounding Urmia Lake was removed from GRACE-TWS using GLDAS data, which is shown as the solid-black line in Fig. 3,A. Our result of surface WS changes from GRACE is comparable, in terms of cycles and trend, with those of Crétaux et al. (2011) for Lake Urmia (the solid-gray line in Fig. 3,A), derived from altimetry and imagery products (http://www.legos.obs-mip.fr/soa/hydrologie/hydroweb/ StationsVirtuelles/SV_Lakes/Urmia.html).

WS change of the Caspian Sea from GRACE products is shown by the solid-black line in Fig. 3,B. For computing the averaged surface WS changes over the Caspian Sea, the average value of steric corrected SSHs was multiplied by the surface area of the sea and is shown by the solid-gray line in Fig. 3,B. The correlation coefficient between the two curves is 0.81, at 95% confidence level, indicating a good agreement. However, in some years (e.g., 2004 and 2008), there are observable differences between the estimated amplitude of the annual WS signal from GRACE and altimetry. This could be due to the steric correction or due to the errors in altimetry data itself. Such observed inconsistencies motivated the introduced approach for separating GRACE-TWS signals.

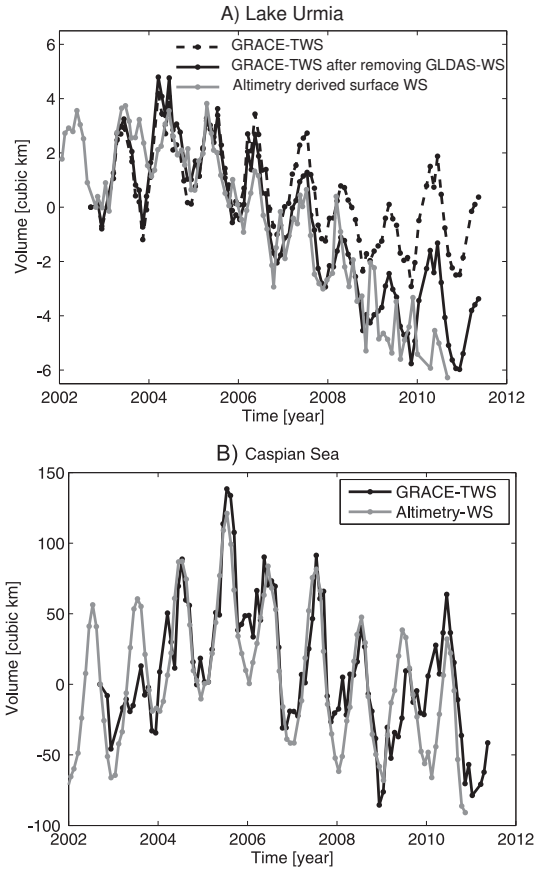

Figure 3: Surface WS changes derived from GRACE and altimetry data, for (A) Lake Urmia and (B) the Caspian Sea. For computing the volume (y-axis), the mean surface area of the Caspian Sea and Urmia Lake (Section 2.3) are multiplied by the mean columns WS changes derived from GRACE and altimetry. During the computations, the shrinking area of Lake Urmia is also taken into account (see also Crétaux et al., 2011).

5.2. Separation (Adjustment) Results

The RMS of GRACE-TWS signals in Fig. 2,A clearly demonstrates the leakage problem. For instance, a part of the Caspian Sea's WS leaked into its surrounding terrestrial signal or vice versa. In order to separate GRACE-TWS changes, we first extracted independent components of WS changes from altimetry and GLDAS outputs. The results are shown and described in Figs. A1, A2, A3, A4 and A5 of Appendix A. The spatial patterns of the mentioned figures were postulated as known patterns in Eq. 4. We also added four other independent components from GLDAS data to Eq. 4. Note that, in order to restrict the length of the paper, spatial patterns of IC3 to IC6 are not shown in Appendix A. The adjusted temporal patterns of surface and terrestrial WS changes are computed using Eq. 4 and are shown in Figs. 4 and 5, respectively. In this paper, the temporal components are scaled by their standard deviations to be unit-less. Spatial patterns of the figures in Appendix A and B are scaled by the standard deviations of their corresponding temporal components to represent anomaly maps of WS in millimeter.

From the annual patterns of surface WS changes, i.e. Fig. 4, A, C, E and F, the amplitude of the adjusted signals are comparable to those of altimetry derived surface WS (EWH) changes. Comparing the adjusted inter-annual changes of surface WS changes (the black lines in Fig. 4,B and D) to their altimetry-derived estimates (the red lines in Fig. 4,B and D) shows that the adjusted values (i.e. coming from GRACE products) are smoother compared to the altimetry results. This is also true for the annual component of the Aral Sea (compare the red and black lines in Fig. 4,E). Investigating the reason for this difference may be the subject of future research.

From the adjusted results, we estimate the amplitude of annual surface WS changes of the Caspian Sea to be 150 mm, whereas amplitudes of 101 mm and 71mm are obtained for the Persian and Oman Gulfs, respectively. Fig. 4, E indicates a negative linear trend of $\sim$20 mm/yr during 2002 to 2011 over the Aral Sea.

IC1 in Fig. 5,A compares the adjusted value of annual terrestrial WS changes with the WS output of GLDAS. Although, the phase of the signal is comparable, the amplitudes of the signal differ over the years. For instance, an attenuation of the annual amplitudes in the years 2008 and 2009, derived from GRACE (the red line in the temporal pattern of IC1) could be related to the prolonged drought condition over Iran (Shean, 2008). This impact is not fully reflected in the GLDAS outputs (the black line in Fig. 5,A). IC2 of GLDAS (the black line in Fig. 5,B) shows an overall decline of terrestrial WS changes mainly over the central and north-western parts of Iran (see the spatial map of IC2 in Fig. A5). The adjusted value of IC2 (the red line in Fig. 5,B) shows that the drought trend actually starts from 2005. The adjusted results are more consistent with the drought behaviour we found for the small lakes of the country and also in-situ observations, with all showing a decline after 2005. We estimate an average decline of 15 mm/yr water column during 2005 to 2011 over central Iran.

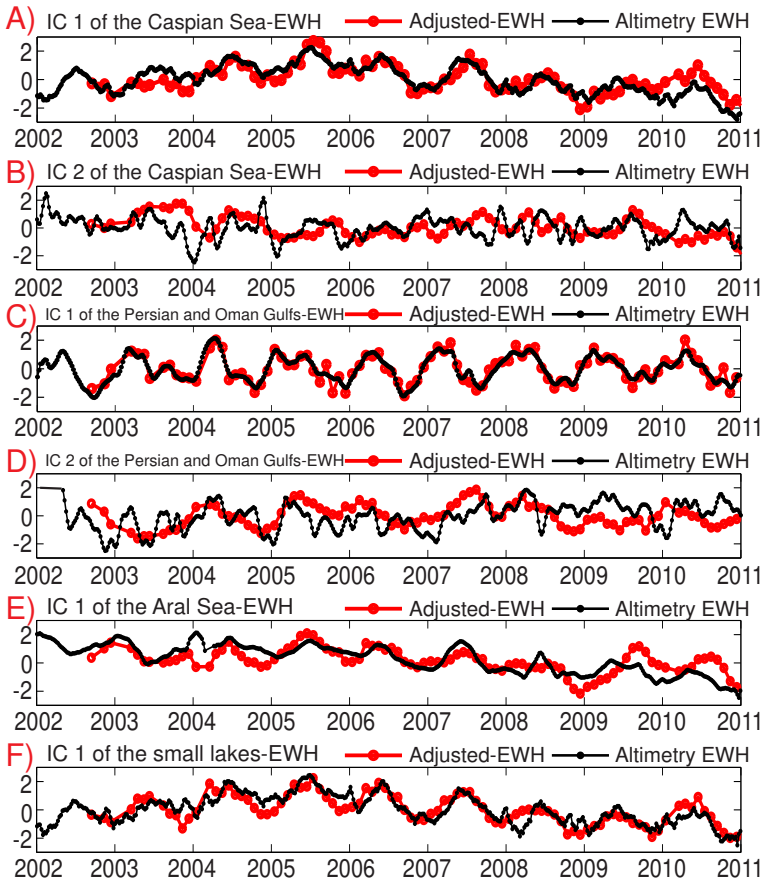

Figure 4: An overview of the adjusted and altimetry derived surface WS changes, shown here in equivalent water height (EWH). The red lines are derived using the LSA method of Section 4 and the black lines are derived from the ICA decomposition of altimetry derived surface WS changes (see Appendix A). (A,B) the first two independent components of the Caspian Sea; (C,D) the first two independent components of the Persian and Oman Gulfs; (E) the first independent component of the Aral Sea; and (F) the first independent component of the small lakes. The temporal patterns are unit-less. The corresponding spatial patterns of (A,B) are shown in Fig. A1; those of (C,D) in Fig. A2; the spatial pattern of (E) in Fig. A3; and that of (F) in Fig. A4. The independent modes are ordered with respect to the variance fraction they represent.

5.3. Comparison of the Adjusted Results with In-situ Observations

Once the signals of the surface and terrestrial WS changes have been separated and their amplitudes are adjusted to the GRACE observations, we use the spatial base-functions derived from GLDAS (i.e. spatial maps of Fig. A5 and 4 other maps that are not shown in the paper) along with their corresponding adjusted temporal values (the red lines in Fig. 5 and 4 others) in Eq. 2 to reconstruct terrestrial WS changes over Iran. In Eq. 2, the spatial maps stored in $\mathbf{A}_H$ and $\mathbf{C}_H$ contain the adjusted temporal components. The RMS and linear

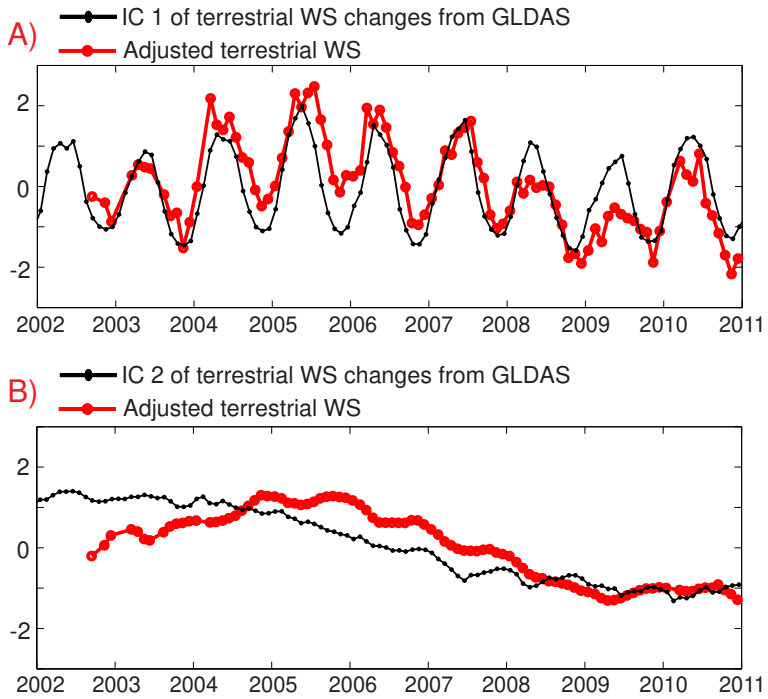

Figure 5: An overview of the main temporal variations of terrestrial WS changes over Iran. The red lines are derived using the LSA method of Section 4 and the black lines are derived from ICA decomposition of GLDAS terrestrial WS changes. (A) corresponds to the first leading independent component, and (B) to the second independent component. The temporal patterns are unit-less and their corresponding spatial patterns are shown in Fig. A5.

trends of the reconstructed signals are shown in Fig. 6,A and B, respectively. The RMS shows that the separation was successful, where for example, the leakage caused by the Caspian Sea signal is removed (compare Fig. 6,A with Fig. 2,A). The linear trends (Fig. 6,B) show a decline in most parts of the country including the northwest, central, as well as over the Zagros chain.

We removed the above reconstructed results from GRACE-TWS maps and compared the results with available in-situ groundwater observations. Before, comparison, each month of the available stations was first smoothed using a Gaussian filter of 400 km radius (Jekeli, 1981). The radius of 400 km was selected to be approximately consistent with the DDK2 filter applied to GRACE-TWS data. We compared the magnitude of the basin averages of the filtered in-situ observations with those we derived from the original values (in Fig. 1). We found a mean damping factor of ~ 0.71, which shows the impact of the GRACE-like post processing on the true in-situ signals. A comparison of the results is shown in Fig. 7. The basin averages derived from both in-situ and satellite observations are consistent in terms of the seasonal peaks and phases. The linear rates of the water storage changes are depicted in Fig. 7 (dash lines).

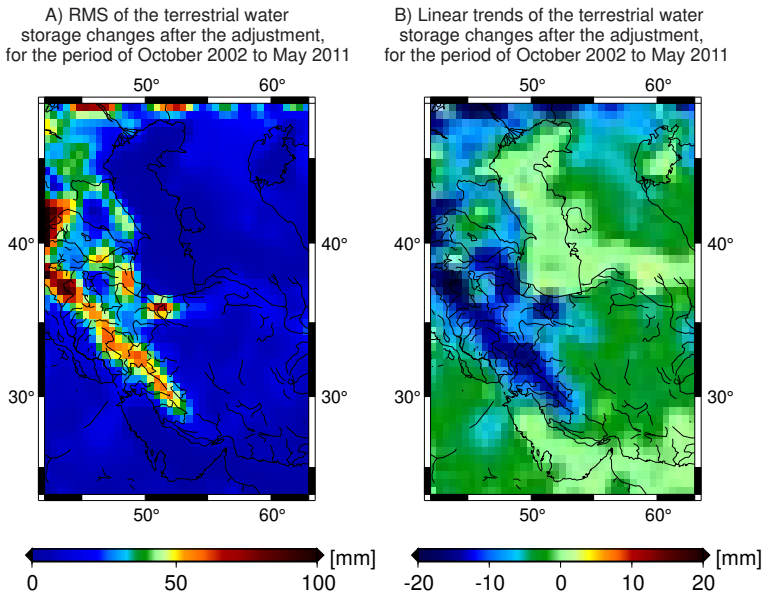

Figure 6: An overview of the reconstructed terrestrial water storage changes over Iran. (A) the RMS of the terrestrial TWS changes after adjusting GRACE-TWS changes (cf. Fig. 2,A) to the base-functions of GLDAS-derived terrestrial WS changes, and (B) the linear trends of the signal in (A).

Basins:	Khazar (Basin 1)	Gulfs (Basin 2)	Urmia (Basin 3)	Markazi (Basin 4)	Hamoon (Basin 5)	Sarakhs (Basin 6)
Groundwater rate of 2003-2005 [mm/yr]:	8.6	5.1	8.5	2.5	1.3	3.7
Groundwater rate of 2005-2011 [mm/yr]:	-6.7	-6.1	-11.2	-9.1	-3.1	-4.2

Table 1: Basin average trends of groundwater variations over the six main basins of Iran derived from GRACE products.

As the figure illustrates, in most of the basins, GRACE derived basin averages tend to show steeper slopes compared to the in-situ observations. Part of this inconsistency might be the result of network changes in a number of stations. We removed those stations from our basin average computations and the new results turned out to be more consistent with that of GRACE (solid gray lines). The other part of inconsistency might be due to our limited knowledge about the porosity parameters used for converting piezometer observations to storage values, which can be quite large for some basins (see e.g., Jiménez-Martínez et al., 2013). Further research, e.g., involving permanent GPS stations, needs to be undertaken to address the problem over the selected region. The results of GRACE-derived groundwater rates are summarized in Table 1.

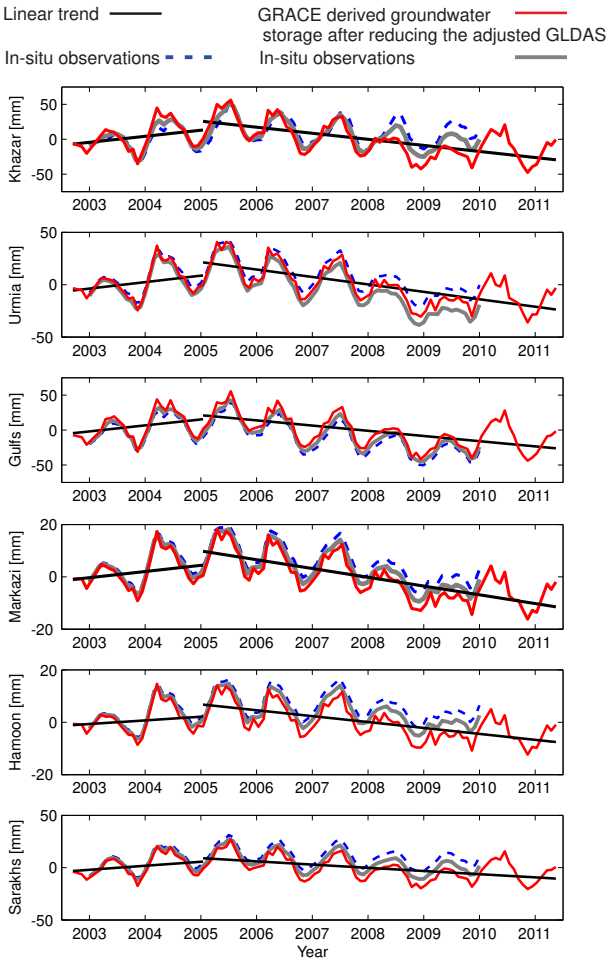

Figure 7: Basin averages of groundwater changes over the six major basins of Iran. The red lines are basin averages after removing the adjusted terrestrial and surface WS changes from GRACE-TWS. The blue dashed lines are derived from in-situ piezometric observations that are located in each basins, respectively. Solid gray lines are derived from the stations, that do not exhibit network changes. Linear trends are shown by the black lines and their rates are reported in Table 1.

6. Conclusion and Outlooks

The water resources in Iran as a part of the Middle-East region are inherently scarce as a result of naturally arid climatic conditions. Population increase and economic growth have spurred higher demands for the limited water resources (FAO, 2009). Therefore, it is desirable to develop monitoring and analysis tools to aid understanding the hydrological cycle of the region. In this context, this study investigated large scale GRACE-TWS pattern changes over a rectangular region that included Iran for the period from October 2002 to March 2011. The extracted patterns are important since GRACE-TWS changes represent integral measurements of water in the entire region. Spatio-temporal changes of TWS, therefore, may be used to study natural and man-made impacts on the regional climate.

In order to deal with the leakage problem of GRACE products and also

to separate terrestrial from surface WS changes, a least squares adjustment approach was applied on the ICA-decomposed terrestrial and surface WS variations respectively from GLDAS and altimetry WS outputs. The applied method, only relies on the ICA-derived spatial patterns of the hydrological model and altimetry observations, which remain invariant in the adjustment. In the adjustment step, the temporal components are estimated from GRACE-TWS data (Section 5.2). Adjusted terrestrial WS over Iran showed an overall declining trend over the country (Fig. 6,B). In Section 5.3, we demonstrated that the estimated groundwater storages are in a good agreement with in-situ piezometric observations. Furthermore, for the first time, this study offers GRACE-derived basin averaged groundwater changes for the six main basins of Iran (basins are selected according to FAO, 2009). Our estimates of the linear trends of WS changes for the period of 2003 to 2005 and the drought period of 2005 to 2011.3 are shown in Table 1. In view of the low availability of renewable water resources in all the basins, in particular, the Markazi and Urmia basins, the results may be an important incentive for the water resource management of Iran. Note that the area of some of our processed basins, for instance Urmia and Sarakhs, are relatively small and might not meet the nominal resolution of the GRACE-TWS products. However, the strong WS signal of the basins and the proposed optimal processing method allowed retrieval of water storage variations.

At the root of the presented separation procedure lies the ICA-decomposition of the GLDAS and altimetry outputs. Such decompositions contain errors as a result of the short length of observations, as well as the errors of observations themselves. Including those errors in the least squares procedure may potentially improve the results but falls outside the scope of the current research. The performed separation approach has the potential to be improved by adding extra information on the patterns of water storage variations over the Mesopotamia region, which covers the Tigris/Euphrates River system, Lake Van etc., (see e.g., Voss et al., 2013). The contribution of such base-functions in the inversion will, however, be marginal and concentrated over the basins located at the west part of the country (i.e. basins 2 and 3). The relationship between WS changes in the six major basins of Iran and climate variability such as decadal rainfall anomalies and large scale ocean-atmospheric patterns of e.g., the El Niño Southern Oscillation phenomenon might be helpful for understanding the water cycle of the region.

Acknowledgement

The authors thank the editor M. Bauer and the anonymous reviewer for the helpful remarks, which improved the manuscript considerably. E. Forootan and J. Kusche are grateful for the financial support provided by the German Research Foundation (DFG) under the project BAYES-G. E. Forootan thanks L. Moxey (the Operations Manager of NOAA OceanWatch - Central Pacific) for the fruitful discussions on altimetry of the Caspian Sea. He also thanks L. Longuevergne (Université de Rennes1) for his useful comments on the performed investigations. The authors also thank Y. Hemmati (Iranian Water-resource

Research Center) for providing the in-situ observations. We are grateful for the satellite and model data used in this study. This is a TIGeR Publication no. 491.

Abbaspour, K.C., Faramarzi, M., Seyed Ghasemi, S., & Yang, H. (2009). Assessing the impact of climate change on water resources in Iran. Water Resources Research, 45, W10434, doi:10.1029/2008WR007615.

Ardakani, R. (2009). Overview of Water Management in Iran. Proceeding of Regional Center on Urban Water Management, Tehran, Iran.

Avsar, N.B., & Ustun, A. (2012). Analysis of regional time-variable gravity using GRACE's 10-day solutions. FIG Working Week 2012, Knowing to manage the territory, protect the environment, evaluate the cultural heritage, Rome, Italy, 6-10 May 2012, http://www.fig.net/pub/fig2012/papers/ts04b/TS04B_avsar_ustun_5724.pdf. (accessed date: May 2013)

Awange, J.L., Fleming, K.M., Kuhn, M., Featherstone, W.E., Heck, B., & Anjasmara, I. (2011). On the suitability of the $4^{\circ} \times 4^{\circ}$ GRACE mascon solutions for remote sensing Australian hydrology. Remote Sensing of Environment, 115, 864-875. doi: 10.1016/j.rse.2010.11.014.

Awange, J., Forootan, E., Kusche, J., Kiema, J.K.B., Omondi, P., Heck, B., Fleming, K., Ohanya, S., & Gonçalves, R.M. (2013). Understanding the decline of water storage across the Ramser-lake Naivasha using satellite-based methods. Advances in Water Resources, 60, 7-23, doi:10.1016/j.advwatres.2013.07.002.

Bari-Abarghouei, H., Asadi-Zarch, M.A., Dastorani, M.T., Kousari, M.R., & Safari-Zarch, M. (2011). The survey of climatic drought trend in Iran. Stochastic Environmental Research and Risk Assessment, 25 (6), 851-863, doi:10.1007/s00477-011-0491-7.

Baur, O., Kuhn, M., & Featherstone, W.E. (2013). Continental mass change from GRACE over 2002-2011 and its impact on sea level. Journal of Geodesy, 87 (2), 117-125, doi:10.1007/s00190-012-0583-2.

Becker, M., Llovel, W., Cazenave, A., Güntner, A., & Crétaux, J.-F. (2010). Recent hydrological behavior of the East African great lakes region inferred from GRACE, satellite altimetry and rainfall observations. Comptes Rendus Geoscience, 342(3), 223-233. http://dx.doi.org/10.1016/j.crte.2009.12.010.

Birkett, C.M. (1995). The global remote sensing of lakes, wetlands and rivers for hydrological and climate research, in Geoscience and Remote Sensing Symposium, 1995. IGARSS 95. 'Quantitative Remote Sensing for Science and Applications', Vol 3, 1979-1981.

Cardoso J.F., & Souloumiac, A. (1993). Blind beamforming for non-Gaussian signals. In: IEEE proceedings, 362370. doi:10.1.1.8.5684.

Chambers, D.P. (2006). Observing seasonal steric sea level variations with GRACE and satellite altimetry. J Geophys Res, 111, C03010, doi:10.1029/2005JC002914.

Cheng, M., & Tapley, B.D. (2004). Variations in the Earth's oblateness during the past 28 years. J Geophys Res, 109, B09402, doi:10.1029/2004JB003028.

Crétaux, J-F., Jelinski, W., Calmant, S., Kouraev, A., Vuglinski, V., Bergé Nguyen, M., Gennero, M-C., Nino, F., Abarca Del Rio, F., Cazenave, A., & Maisongrande, P. (2011). SOLS: A lake database to monitor in near real time water level and storage variations from remote sensing data, Journal of Advanced Space Research, 1497-1507, doi:10.1016/j.asr.2011.01.004.

Duan, J., Shum, C.K., Guo, J., & Huang, Z. (2012). Uncovered spurious jumps in the GRACE atmospheric de-aliasing data: potential contamination of GRACE observed mass change. Geophys. J. Int., 191, 83-87, doi:10.1111/j.1365-246X.2012.05640.x.

FAO, (2009). FAO Water Report 34.

Farrell, W. E., & Clark, J. A. (1976). On postglacial sea level. Geophysical Journal of the Royal Astronomical Society, 46(3), 647-667.

Famiglietti, J.S., Rodell, M. (2013). Water in the balance. Science 340 (6138), 1300-1301, doi:10.1126/science.1236460.

Fenoglio-Marc, L., Kusche, J., & Becker, M. (2006). Mass variation in the Mediterranean Sea from GRACE and its validation by altimetry, steric and hydrologic fields. Geophysical Research Letters, 33(19), doi:10.1029/2006GL026851.

Fenoglio-Marc, L., Rietbroek, R., Grayek, S., Becker, M., Kusche, J., & Stanev, E. (2012). Water mass variation in the Mediterranean and Black Sea. Journal of Geodynamics, 59-60, 168-182, http://dx.doi.org/10.1016/j.jog.2012.04.001.

Flechtner, F. (2007a). AOD1B product description document for product releases 01 to 04. Technical Report, Geoforschungszentrum (GFZ), Potsdam.

Flechtner, F. (2007b). GFZ Level-2 processing standards document for level-2 product release 0004, GRACE 327-743, Rev. 1.0. Technical Report, Geoforschungszentrum, Potsdam.

Forootan, E., Awange, J., Kusche, J., Heck, B., & Eicker, A. (2012), Independent patterns of water mass anomalies over Australia from satellite data and models. Remote Sensing of Environment, 124, 427-443, doi:0.1016/j.rse.2012.05.023.

Forootan, E., & Kusche, J. (2013). Separation of deterministic signals, using independent component analysis (ICA). Stud. Geophys. Geod, Vol.57 (1), 17-26, doi: 10.1007/s11200-012-0718-1.

Forootan, E., & Kusche, J. (2012). Separation of global time-variable gravity signals into maximally independent components. Journal of Geodesy, 86 (7), 477-497, doi:10.1007/s00190-011-0532-5.

Forootan, E., Didova, O., Kusche, J., & Löcher, A. (2013). Comparisons of atmospheric data and reduction methods for the analysis of satellite gravimetry observations. JGR-Solid Earth, doi: 10.1002/jgrb.50160.

Frappart, F., Ramillien, G., Leblanc, M., Tweed, S.O., Bonnet, M.P., & Maisongrande, P. (2010). An independent component analysis filtering approach for estimating continental hydrology in the GRACE gravity data. Remote Sens Environ, 115(1), 187-204. doi:10.1016/j.rse.2010.08.017

Ghandhari, A., & Alavi-Moghaddam, S.M.R. (2011). Water balance principles: A review of studies on five watersheds in Iran. Journal of Environmental Science and Technology, 4 (5), 465-479, ISSN: 1994-7887, doi:10.3923/jest.2011.465.479.

Grippa, M., Kergoat, L., Frappart, F., Araud, Q., Boone, A., de Rosnay, P., Lemoine, J.-M., Gascoin, S., Balsamo, G., Ottlé, C., Decharme, B., Saux-Picart, S., & Ramillien, G. (2011), Land water storage variability over West Africa estimated by Gravity Recovery and Climate Experiment (GRACE) and land surface models. Water Resour. Res., 47, W05549, doi:10.1029/2009WR008856.

Güntner, A., Stuck, J., Werth, S., Döll, P., Verzano, K., & Merz, B. (2007). A global analysis of temporal and spatial variations in continental water storage. Water Resour. Res., 43, W05416, doi:10.1029/2006WR005247.

Güntner, A. (2008). Improvement of global hydrological models using GRACE data, Surv. Geophys., 29, 375-397.

Ishii, M., & Kimoto. M. (2009). Reevaluation of historical ocean heat content variations with time-varying XBT and MBT depth bias corrections. Journal of Oceanography 65, 287-299.

Jekeli, C. (1981). Alternative methods to smooth the Earth's gravity field. Technical report rep 327. Department of Geodesy and Science and Surveying, Ohio State University, Columbus.

Jensen, L., Rietbroek, R., & Kusche, J. (2013). Land water contribution to sea level from GRACE and Jason-1 measurements. Journal of Geophysical Research-Oceans, 118 (1), 212226, doi:10.1002/jgrc.20058.

Jiménez-Martínez, J., Longuevergne, L., Le Borgne, T., Davy, P., Russian, A., & Bour, O. (2013). Temporal and spatial scaling of hydraulic response to recharge in fractured aquifers: Insights from a frequency domain analysis. WATER RESOURCES RESEARCH, 49, 1-17, doi:10.1002/wrcr.20260.

Kampf, J., & Sadrinasab, M. (2006). The circulation of the Persian Gulf: a numerical study. Ocean Sci., 2, 27-41. http://www.ocean-sci.net/2/27/2006/os-2-27-2006.html.

Klees, R., Revtova, E.A., Gunter, B.C., Ditmar, P., Oudman, E., Winsemius, H.C. & Savenije, H.H.G. (2008). The design of an optimal filter for monthly GRACE gravity models. Geophysical Journal International, 175(2), 417-432, doi:10.1111/j.1365-246X.2008.03922.x.

Klees, R., Zapreeva, E.A., Winsemius, H.C., & Savenije, H.H.G. (2007). The bias in GRACE estimates of continental water storage variations. Hydrology and Earth System Sciences Discussions, 11, 1227-1241.

Koch, K.R. (1988). Parameter estimation and hypothesis testing in linear models. Springer, New York. ISBN:978354065257.

Kosarev, A.N., & Yablonskaya, E.A., (1994). The Caspian Sea. The Netherlands:SPB Academic Publishing, pp. 260, ISBN-10:9051030886.

Kouraev, A.V., Crétaux, J.-F., Lebedev, S.A., Kostianoy, A.G., Ginzburg, A.I., Sheremet, N.A., Mamedov, R., Zakharova, E.A., Roblou, L., Lyard, F., Calmant, S., & Berge-Nguyen, M. (2011). Satellite altimetry applications in the Caspian Sea (Chapter 13). In Coastal Altimetry, (Eds) S., Kostianoy, A., Cipollini, P., and Benveniste, J. Springer, 331-366, ISBN:978-3-642-12795-3.

Kusche, J. (2007). Approximate decorrelation and non-isotropic smoothing of time-variable GRACE-type gravity field models. Journal of Geodesy, 81, 733-749, doi:10.1007/s00190-007-0143-3.

Kusche, J., Klemann, V., & Bosch, W. (2012). Mass distribution and mass transport in the Earth system. Journal of Geodynamics, 59-60, 1-8, http://dx.doi.org/10.1016/j.jog.2012.03.003.

Kusche, J., Schmidt, R., Petrovic, S., & Rietbroek, R. (2009). Decorrelated GRACE time-variable gravity solutions by GFZ, and their validation using a hydrological model. Journal of Geodesy, 83, 903-913, doi:10.1007/s00190-009-0308-3.

Lambeck, K., Esat, T.M., & Potter, E.K. (2002). Links between climate and sea levels for the past three million years. Nature., 2002 Sep 12, 419(6903), 199-206.

Llovel, W., Becker, M., Cazenave, A., Crétaux, J-F., & Ramillien, G. (2010). Global land water storage change from GRACE over 2002-2009; Inference on sea level. Comptes Rendus Geoscience, 342, (3), 179-188, doi:http://dx.doi.org/10.1016/j.crte.2009.12.004.

Longuevergne, L., Scanlon, B.R., & Wilson, C.R. (2010). GRACE Hydrological estimates for small basins: Evaluating processing approaches on the High Plains Aquifer, USA. Water Resources Research, 46 (11), W11517, doi:10.1029/2009WR008564.

Longuevergne, L., Wilson, C.R., Scanlon, B.R., & Crétaux, J-F. (2012). GRACE water storage estimates for the Middle East and other regions with significant reservoir and lake storage. Hydrol. Earth Syst. Sci. Discuss., 9, 11131-11159, doi:10.5194/hessd-9-11131-2012.

Modarres, R. (2006). Regional precipitation climates of Iran. Journal of Hydrology (NZ) 45 (1), 13-27, ISSN:0022-1708.

Mohammadi-Ghaleni, M., & Ebrahimi, K. (2011). Assessing impact of irrigation and drainage network on surface and groundwater resources - case study: Saveh Plain, Iran. ICID 21'st International Congress on Irrigation and Drainage, 15-23 October 2011, Tehran, Iran.

Motagh, M., Walter, T. R., Sharifi, M. A., Fielding, E., Schenk, A., Anderssohn, J., & Zschau, J. (2008). Land subsidence in Iran caused by widespread water reservoir overexploitation. Geophysical Research Letters, 35, L16403, doi:10.1029/2008GL033814.

Noory H., van der Zee, S.E.A.T.M., Liaghat, A.-M., Parsinejad, M., & van Dam, J.C. (2011). Distributed agro-hydrological modeling with SWAP to improve water and salt management of the Voshmgir irrigation and drainage network in Northern Iran. Agricultural Water Management, 98, 1062-1070, doi:10.1016/j.agwat.2011.01.013.

Pous, S.P., Carton, X., & Lazure, P. (2004). Hydrology and circulation in the Strait of Hormuz and the Gulf of Oman, Results from the GOGP99 Experiment: 2. Gulf of Oman. Journal of Geophysical Research, 109, C12038, doi:10.1029/2003JC002146.

Preisendorfer, R. (1988). Principal component analysis in Meteorology and Oceanography. Elsevier: Amsterdam, 426 pages. ISBN:0444430148.

Ramillien, G., Famiglietti, J.S., & Wahr, J. (2008). Detection of continental hydrology and glaciology signals from GRACE: a review, Surv. Geophys., 29, 361-374, doi:10.1007/s10712-008-9048-9.

Reynolds, R.W., Rayne, N.A., Smith, T.M., Stokes, D.C., & Wang, W. (2002). An improved in situ and satellite SST analysis for climate. J. Clim., 15 (2002), pp. 1609-1625.

Rietbroek, R., Brunnabend, S.E., Dahle, C., Kusche, J., Flechtner, F., Schröter, J., & Timmermann, R. (2009). Changes in total ocean mass derived from GRACE, GPS, and ocean modeling with weekly resolution. J Geophys Res., 114, C11004, doi:10.1029/2009JC005449.

Rietbroek, R., Brunnabend, S.E., Kusche, J., & Schröter, J. (2012). Resolving sea level contributions by identifying fingerprints in time-variable gravity and altimetry. Journal of Geodynamics, 59, 72-81, http://dx.doi.org/10.1016/j.jog.2011.06.007.

Rodell, M., Chen. J., Kato, H., Famigietti, J., Nigro, J., & Wilson, C. (2007). Estimating ground water storage changes in the Mississippi River basin (USA) using GRACE. Hydrogeol. J. 15 159-166. doi:10.1007/s10040-006-0103-7.

Rodell, M., & Famiglietti, J.S. (2001), An analysis of terrestrial water storage variations in Illinois with implications for the Gravity Recovery and Climate Experiment (GRACE), Water Resour. Res., 37(5), 1327-1340, doi:10.1029/2000WR900306.

Rodell, M., Houser, P.R., Jambor, U., Gottschalck, J., Mitchell, K., Meng, K., Arsenault, C.-J., Cosgrove, B., Radakovich, J., Bosilovich, M., Entin, J.K., Walker, J.P., Lohmann, D., & Toll, D. (2004). The Global Land Data Assimilation System. Bulletin of the American Meteorological Society, 85 (3), 381-394.

Rodell, M., Velicogna, I., & Famiglietti, J.S. (2009). Satellite-based estimates of groundwater depletion in India. Nature, 460, 999-1002, doi:10.1038/nature08238.

Sarraf, M., Owaygen, M., Ruta, G., & Croitoru, L. (2005). Islamic Republic of Iran: Cost assessment of environmental degradation, Tech. Rep. 32043-IR, World Bank, Washington, D. C.

Schmeer, M., Schmidt, M., Bosch, W., & Seitz, F. (2012). Separation of mass signals within GRACE monthly gravity field models by means of empirical orthogonal functions. Journal of Geodynamics, 59-60, 124-132, doi:10.1016/j.jog.2012.03.001.

Schmidt, M., Seitz, F., & Shum, C.K. (2008). Regional fourdimensional hydrological mass variations from GRACE, atmospheric flux convergence, and river gauge data, J. Geophys. Res., 113, B10402, doi:10.1029/2008JB005575.

Schnitzer, S., Seitz, F., Eicker, A., Güntner, A., Wattenbach, M., & Menzel, A. (2013). Estimation of soil loss by water erosion in the Chinese Loess Plateau using universal soil loss equation and GRACE. Geophys. J. Int., doi:10.1093/gji/ggt023.

Sharifi, M.A., Forootan, E., Nikkhoo, M., Awange, J., & Najafi-Alamdari, M. (2013). A point-wise least squares spectral analysis (LSSA) of the Caspian Sea level fluctuations, using TOPEX/Poseidon and Jason-1 observations. Advances in Space Research, 51 (5), 858-873, http://dx.doi.org/10.1016/j.asr.2012.10.001.

Shean, M. (2008). IRAN: 2008/09 wheat production declines due to drought. Commodity intelligence report. United States Department of Agriculture (USDA), http://www.pecad.fas.usda.gov/highlights/2008/05/Iran_may2008.html. Access date: 20.02.2013.

Shum, C.K., Jun-Yi, G., Hossain, F., Duan, J., Alsdorf, D.E., Duan, X-J, Kuo, C-Y., Lee, K., Schmift, M., & Wang, L. (2011). Inter-annual Water Storage Changes in Asia from GRACE Data. In R. Lal et al. (eds.), Climate Change and Food Security in South Asia, doi:10.1007/978-90-481-9516-9_6.

720 Swenson, S., & Wahr, J. (2002). Methods for inferring regional surface-mass anomalies from Gravity Recovery
721 and Climate Experiment (GRACE) measurements of time-variable gravity. Journal of Geophysical Research,
722 107 (B9), ETG 3-1 - 3-13, doi:10.1029/2001JB000576.

723 Swenson, S., & Wahr, J. (2006). Post-processing removal of correlated errors in GRACE data. Geophys Res
724 Lett., 33, L08402, doi:10.1029/2005GL025285.

725 Swenson, S., & Wahr, J. (2007). Multi-sensor analysis of water storage variations of the Caspian Sea. Geophys
726 Res Lett., 34, L16401, doi:10.1029/2007GL030733.

727 Syed, T.H., Famiglietti, J.S., Chen, J., Rodell, M., Seneviratne, S.I., Viterbo, P., & Wilson, C.R. (2005).
728 Total basin discharge for the Amazon and Mississippi River basins from GRACE and a land-atmosphere water
729 balance, Geophys. Res. Lett., 32, L24404, doi:10.1029/2005GL024851.

730 Syed, T.H., Famiglietti, J.S., Rodell, M., Chen, J., & Wilson, C.R. (2008). Analysis of terrestrial water storage
731 changes from GRACE and GLDAS, Water Resources Research, 44, W02433, doi:10.1029/2006WR005779.

732 Tapley, B., Bettadpur, S., Ries, J., Thompson, P., & Watkins, M. (2004a). GRACE measurements of mass
733 variability in the Earth system. Science, 305, 503-505. http://dx.doi.org/10.1126/science.1099192.

734 Tapley, B., Bettadpur, S., Watkins, M., & Reigber, C. (2004b). The gravity recovery and cli-
735 mate experiment: Mission overview and early results. Geophysical Research Letters, 31, L09607.
736 http://dx.doi.org/10.1029/2004GL019920.

737 Van Camp, M., Radfar, M., Martens, K., & Walraevens, K. (2012). Analysis of the groundwater resource
738 decline in an intramountain aquifer system in Central Iran. GEOLOGICA BELGICA (2012) 15/3: 176-180.

739 van Dijk, A.I.J.M. (2011) Model-data fusion: using observations to understand and reduce uncertainty in hy-
740 drological models. 19th International Congress on Modelling and Simulation, Perth, Australia, 12-16 December
741 2011. http://mssanz.org.au/modsim2011/index.html

742 van Dijk, A.I.J.M., Renzullo, L.J., & Rodell, M. (2011). Use of Gravity Recovery and Climate Experiment
743 terrestrial water storage retrievals to evaluate model estimates by the Australian water resources assessment
744 system. Water Resour. Res., 47, W11524, doi:10.1029/2011WR010714.

745 Voss, K.A., Famiglietti, J.S., Lo, M-H., de Linage, C., Rodell, M., & Swenson, S.C. (2013). Groundwater
746 depletion in the Middle East from GRACE with implications for transboundary water management in the
747 Tigris-Euphrates-Western Iran region, Water Resour. Res., 49, doi:10.1002/wrcr.20078.

748 Wahr, J., Molenaar, M., & Bryan, F. (1998). Time variability of the Earth's gravity field: Hydrological and
749 oceanic effects and their possible detection using GRACE. Journal of Geophysical Research 103 (B12), 30205-
750 30229, doi:10.1029/98JB02844.

751 Wahr, J., Swenson, S., Velicogna, I., & Zlotnicki, V. (2004). Time-variable gravity from GRACE: First results,
752 Geophysical Research Letters paper 10.1029/2004GL019779.

753 Werth, S., Güntner, A., Schmidt, R., & Kusche, J. (2009). Evaluation of GRACE filter tools from a hy-
754 drological perspective. Geophysical Journal International, 179, 1499-1515, http://dx.doi.org/10.1111/j.1365-
755 246X.2009.04355.x.

Appendix A

Extracting Independent Components from GLDAS and Altimetry WS Changes

ICA is applied on the data sets on each GLDAS and altimetry data sets using Eqs. 2 and 3 (see the details of application in e.g., Forootan and Kusche, 2012). For altimetry products, ICA was individually implemented on (i) the Caspian Sea, (ii) the Persian and Oman Gulfs, (iii) the Aral Sea, and finally (iv) the other small lakes. The results are depicted in Figs. A1, A2, A3 and A4. Note that, similar to the main text, all the temporally independent components (ICs) are unit-less and the spatial patterns are given in millimeters.

Fig. A1 shows the first two independent modes, accounting for 93% of the surface WS variance in the Caspian Sea. The remaining 7% of the variance are noisy and are not shown here. IC1 shows an annual behaviour along with two linear trends, one from January 2002 to December 2005 with a rate of 108 mm/yr and the other from January 2006 to October 2008 with a rate of -152 mm/yr. IC2 indicates the main inter-annual variability from which, the spatial pattern of IC2 shows that the northern part of Caspian exhibits stronger inter-annual variations compared to the central and southern parts (see Fig. A1). This can be related to the climatic extremes, which are more pronounced in the northern part of the Caspian sea inducing stronger mass variations (Kouraev et al., 2011; Sharifi et al., 2013).

The ICA decomposition of WS changes of the Persian and Oman Gulfs also shows two significant components explaining 89% of the total variance. IC1 shows an annual behaviour with a dipole spatial structure over the two gulfs (see Fig. A2, spatial pattern of IC1). IC2 shows a superposition of inter-annual variability and a positive linear trend (9 mm/yr) dominant mainly over the head of the Persian Gulf, where Lambeck et al. (2002) reported a rise due to the post glacial rebound.

Fig. A3 shows that only one of the independent component of surface WS changes (corresponding to 89% of the total variance) over the Aral Sea is statistically significant. IC1 of Aral shows the shrinking of the sea with an average linear rate of 300 mm/yr. Results of ICA, applied on surface WS changes of the small lakes and reservoirs, are shown in Fig. A4. While only the first IC corresponding to 93% of total variance was significant, it shows that most of the surface water of Iran, specifically after the year 2005, are losing water. This situation might be related to the long-term drought condition of the country, see e.g. Bari-Abarghouei et al. (2011).

For brevity we only present the first two independent components of GLDAS data, explaining 71% of the total variance of terrestrial WS changes in Fig. A5. The temporal pattern of IC1 shows the dominant annual variation, while the spatial pattern of IC1 is mainly concentrated over north and west Iran. The temporal pattern of IC2 shows an overall linear trend (during 2002 to 2010) corresponding to a decrease of WS over the Markazi and Urmia Basins (see Fig. A5, spatial pattern of IC2). The derived trend appears to differ from the observations of WS changes, e.g., over Urmia (Fig. 3,A) and other small lakes (Fig. A4), where the WS decrease starts from 2005.

We should mention here, that to reconstruct 90% of the GLDAS data, one needs to select at least the first six independent components of GLDAS. The temporal behaviours of the remaining four independent components of GLDAS were difficult to interpret and are therefore not plotted. These components were, however, still used in the adjustment procedure.

Appendix B

Self-gravitational Impact

The strong seasonal mass fluctuations in the Caspian Sea will cause a time variable change in the geoid. On very short time scales (typically days), the ocean will adapt itself to this new equipotential surface, similar to the tidal response of the ocean. This implies that the sea level in the Gulfs and the Black Sea are (indirectly) influenced by the variations in the Caspian Sea. This effect is known as the self-consistent sea level response and has already been described in Farrel and Clarke (1976). When unaccounted for, this effect may potentially mix signal between the base-functions discussed in the main text. We, therefore, quantified its magnitude by taking the steric corrected sea level from altimetry and computed the self consistent sea level response according to Rietbroek et al. (2012). Fig. B1 shows the RMS of this effect. The effect is strongest in the Black Sea, since it is located closest to the Caspian Sea. However the magnitude of the effect is very small compared to the hydrological and oceanic signal sought such that it is not expected to influence the results.

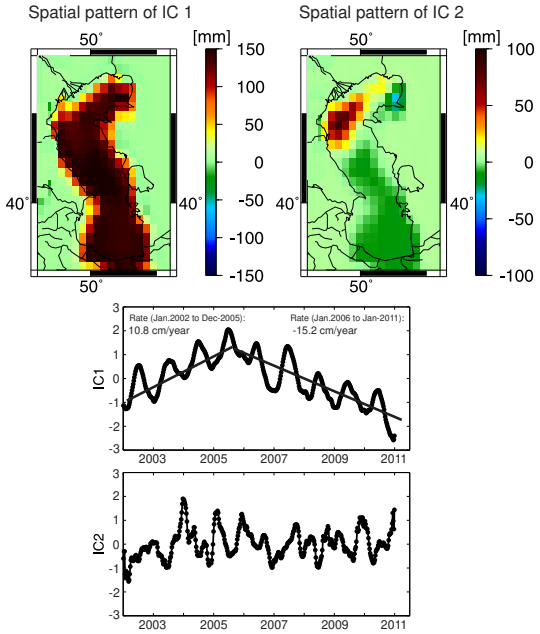

Figure A1: Results of the ICA method applied to the steric corrected SSH data (surface WS changes) over the Caspian Sea. The results are ordered according to their signal strength.

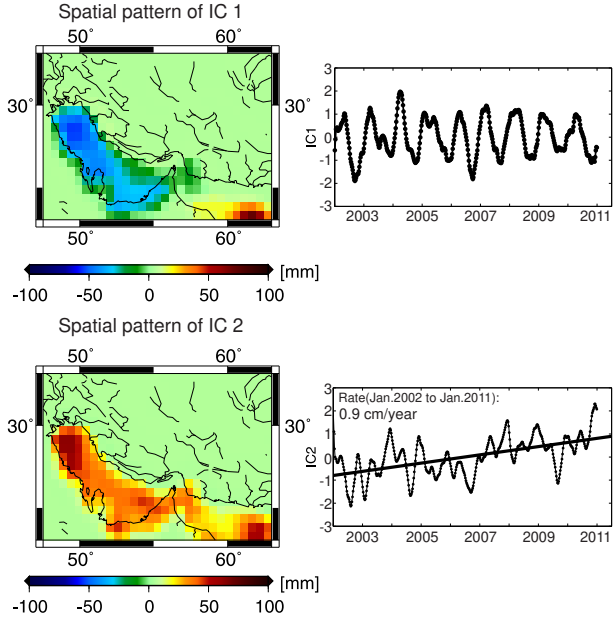

Figure A2: Results of the ICA method applied to the steric corrected SSH data (surface WS changes) over the Persian and Oman Gulfs. The results are ordered according to their signal strength.

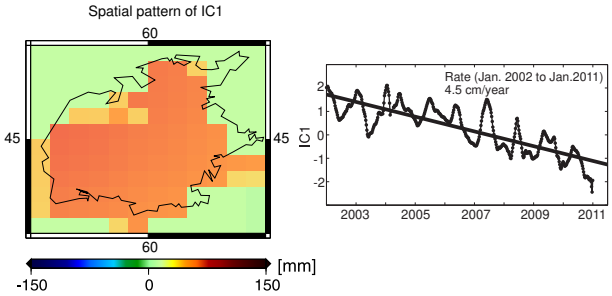

Figure A3: The dominant independent mode of surface WS changes of the Aral Sea.

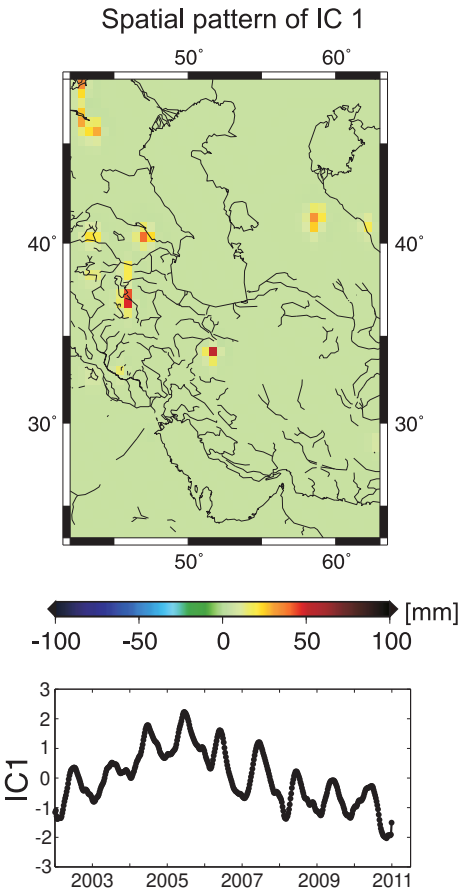

Figure A4: Results of the ICA method applied to the surface WS data over small lakes and reservoirs of the region.

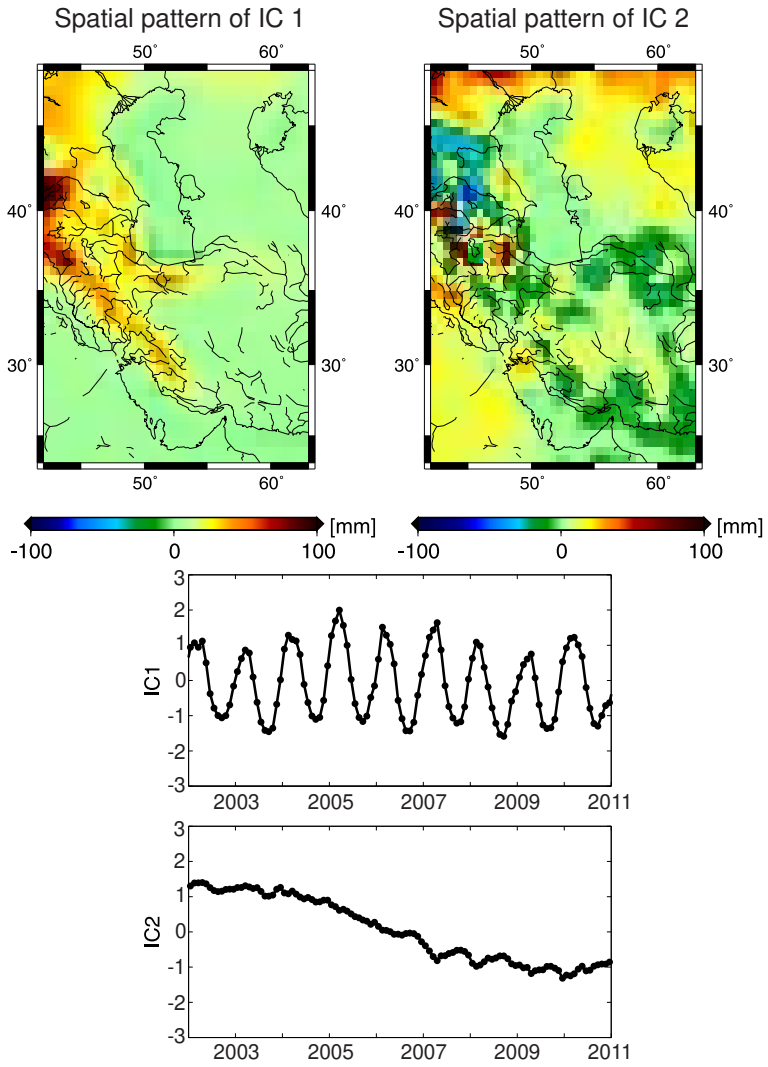

Figure A5: Results of the ICA method applied to the terrestrial WS outputs of the GLDAS model over a rectangular region, including Iran. The components are ordered according to the magnitude of variance they represent.

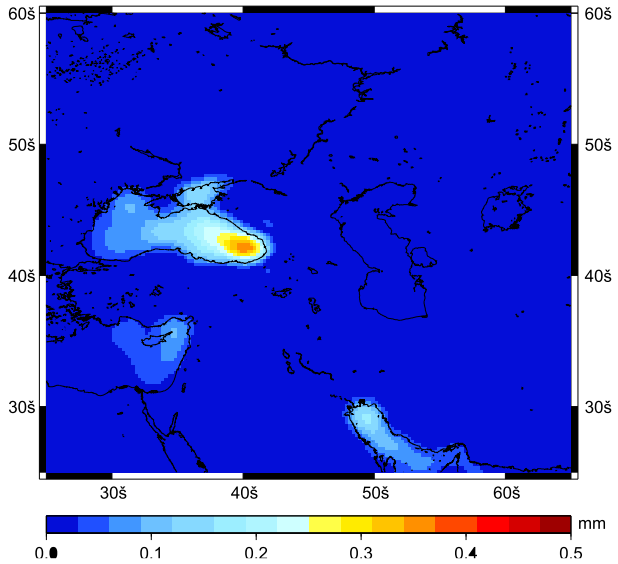

Figure B1: RMS of the self gravitational effect of the Caspian Sea's level variations (steric corrected altimetry) on relative sea level in the Gulfs and the Black Sea.